

Supplementary material

1.1 Enzyme production

AAO of *Pleurotus ostreatus*

(30-L stirred tank)

- Medium: 10.0 g glucose (Merck); 1.0 g Na acetate (Merck); 2.0 g yeast extract (Merck); 5.0 g peptone (from soybeans, Merck); 2.0 g KH_2PO_4 (Merck); 0.5 g $\text{MgSO}_4 \times 7 \text{H}_2\text{O}$ (Merck); 0.1 g CaCl_2 (Merck); 0.01 g $\text{FeSO}_4 \times 7 \text{H}_2\text{O}$ (Merck); pH 5.2
- Aryl alcohol oxidase (AAO, E.C. 1.1.3.7): oxidation of veratryl alcohol to veratraldehyde at pH 5.0 (Kirk et al., 1986); 310 nm ($\epsilon = 9,300 \text{ M}^{-1} \text{ cm}^{-1}$); 50 mM Na citrate (pH 5.0 or 5.5); 5 mM veratryl alcohol

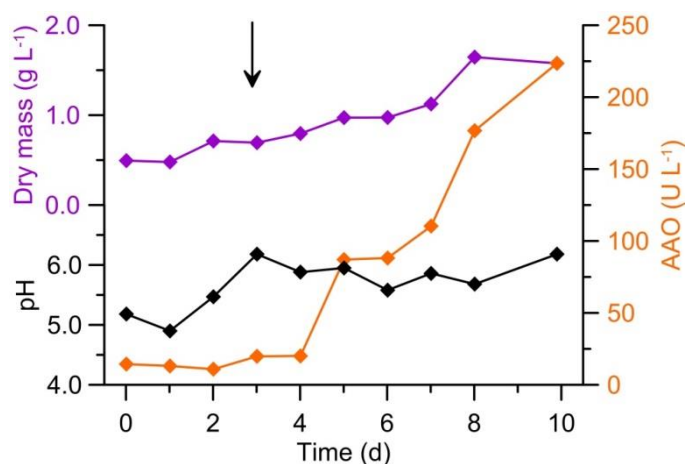


Fig S1: Time course of AAO production by *Bjerkandera adusta* in a stirred-tank bioreactor (with 8 L culture medium); the arrow indicates supplementation with veratryl alcohol to stimulate AAO production. Purple curve - dry mass; black curve - pH; orange curve - PostAAO activity

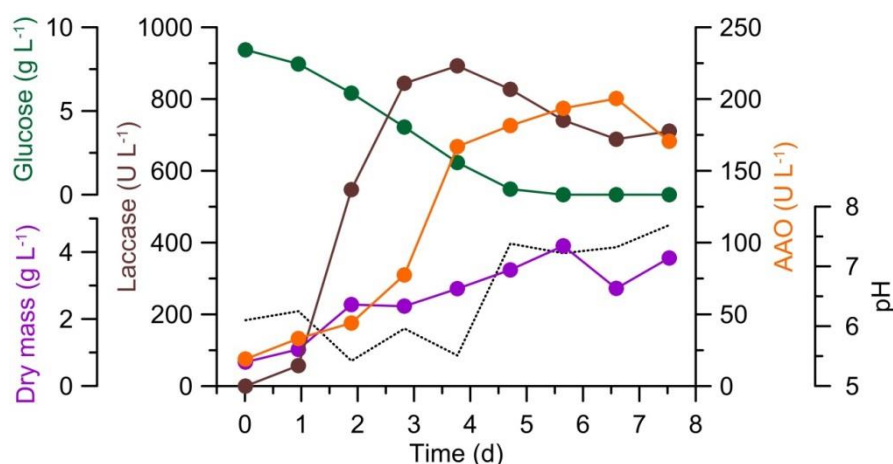


Fig. S2: Time course of AAO production by *Pleurotus ostreatus* in a 30-L stirred tank reactor (20 L medium). Purple curve - dry mass; green curve - glucose concentration; black curve - pH; orange curve - PostAAO activity; brown curve - Laccase Activity

1.2 Enzyme purification

Ion-exchange chromatography:

Sample preparation: dilution with 10 mM Na acetate pH 6.0 (resulting in a pH around 7)

Column: **Q-sepharose**[®], 26 mm x 200 mm, GE Healthcare

Loading buffer: 10 mM Na acetate pH 6.0

Elution buffer: 10 mM Na acetate pH 5.7 + 2 M NaCl

Flow: 13 mL min⁻¹, loading with sample pump; washing with 1.5 CV; 50% B within 10 CV; fraction size 7 mL; around 2,700 U *PostAAO* were applied per run → recovery 2,800 U

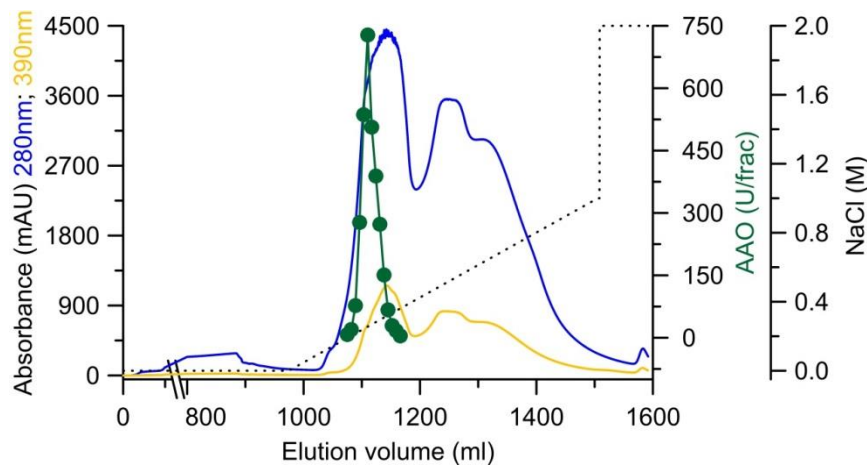


Fig. S3: Elution profile of *PostAAO*; anion exchange chromatography occurred on a Q-sepharose[®] column (26/200) after loading 2,700 U *PostAAO*.

Sample preparation: dilution & purging with 10 mM Na acetate (pH 6) using viva spins: 10 kDa cut-off

Column: **Mono Q**[®], 10 mm x 100 mm, GE Healthcare

Loading buffer: 10 mM Na acetate pH 5.25

Elution buffer: 10 mM Na acetate pH 5.7 + 2 M NaCl

Flow: 6 mL min⁻¹, loading with sample pump; washing with 2.0 CV; 30% B within 15 CV; fraction size 2 mL; around 2,800 U *PostAAO* were applied per run → recovery 2,600 U

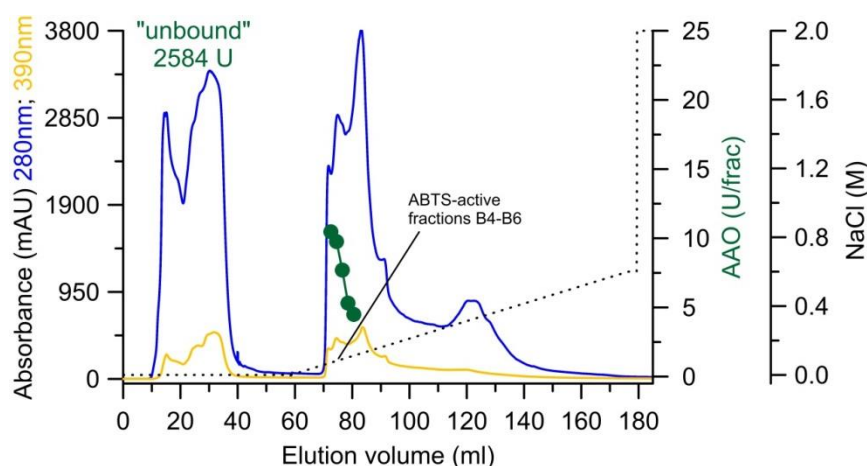


Fig. S4: Elution profile of *PostAAO*; anion exchange chromatography (MonoQ[®] 10/100) after applying 2,800 U *PostAAO*.

Only traces of *PostAAO* bound, probably due to residual salts, but the purification step was nevertheless successful (compare purification table S1). *PostLac*: ABTS oxidizing fractions were pooled (B4-B6), color: bluegreen; "unbound fraction" was concentrated with viva spins: 10 kDa cut-off.

Size exclusion chromatography:

Sample preparation: dilution with SEC buffer and concentration with viva spins (10 kDa cut-off)

Column: **Sephadex[®]75**; 26 mm x 600 mm, GE Healthcare

Buffer: 50 Na acetate, 100 mM NaCl, pH 6.8

Flow: 2.5 mL min⁻¹, loading with a sample loop; fraction size 2 mL

around 2,500 U *Post*AAO were applied in two runs → recovery 2,000 U

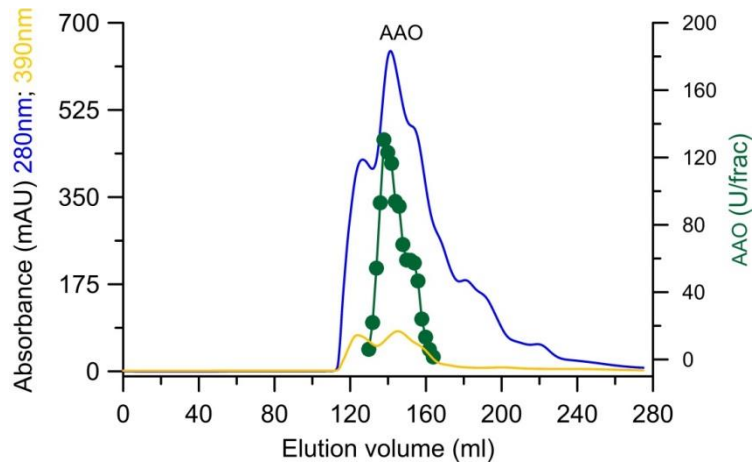


Fig. S5: Elution profile (size exclusion chromatography = SEC) on a Sephadex[®]75 (26/600) column after loading 1,250 U *Post*AAO.

Ion-exchange chromatography:

Sample preparation: dilution & purging with 10 mM Na acetate (pH 6.0) with viva spins (10 kDa cut-off)

Column: **MonoQ**[®], 5 mm x 5 mm, GE Healthcare

Loading buffer: 10 Na acetate, pH 6.0

Elution buffer: 10 Na acetate pH 6.0 + 1 M NaCl

Flow: 2 mL min⁻¹, loading with sample pump; washing with 2.0 CV; 30% B within 35 CV; fraction size 0.8 mL; around 2,500 U *Post*AAO were applied in four runs → recovery 1,600 U

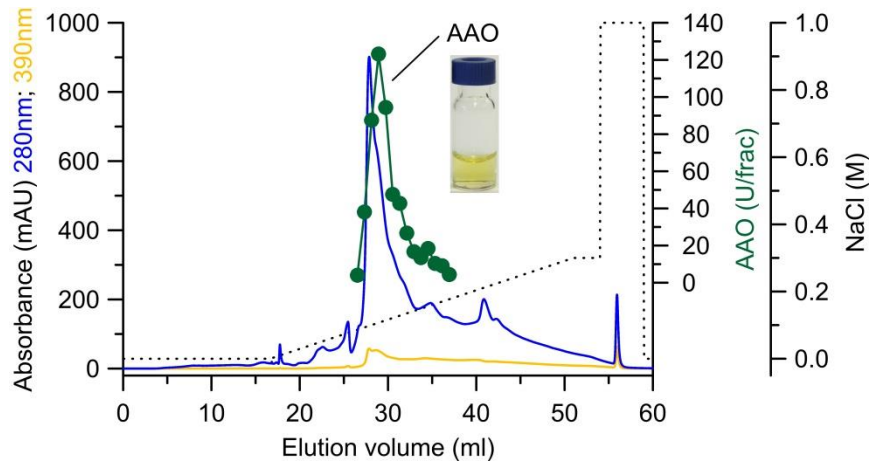


Fig. S6: Elution profile of *Post*AAO (600 U); anion exchange chromatography on MonoQ[®] (5/50).

Protein purification results:

Protein content: Bradford Assay with Roti[®]-Nanoquant, Carl Roth; 200 μ L Roti[®]-Nanoquant + 50 μ L sample in 96-well plates

Activity of aryl alcohol oxidase (AAO, E.C. 1.1.3.7): oxidation of veratryl alcohol to veratraldehyde at pH 5.5; 310 nm ($\epsilon = 9300 \text{ M}^{-1} \text{ cm}^{-1}$); 50 mM Na citrate; 5 mM veratryl alcohol

Tab. S1: Purification of AAO from *Pleurotus ostreatus*

Purification step	Total activity [U]	Total protein [mg]	Specific activity [U mg ⁻¹]	Purification (-fold)	Yield (%)	Volume activity (U mL ⁻¹)	Protein conc. (mg mL ⁻¹)	Volume [mL]
Ultrafiltrate	2,710	615	4.4	1	(100)	3.3	0.75	820
Q-sepharose [®]	2,849	245.2	11.6	3	100	142.5	12.26	20
MonoQ [®] (10/100)	2,584	138.27	18.7	4	95	172.2	9.22	15
Sephadex [®] 75	1,785	47.92	37.2	8	66	223.1	5.99	8
MonoQ [®] (5/50)	1,662	20.63	80.6	18	61	302.3	3.75	5.5

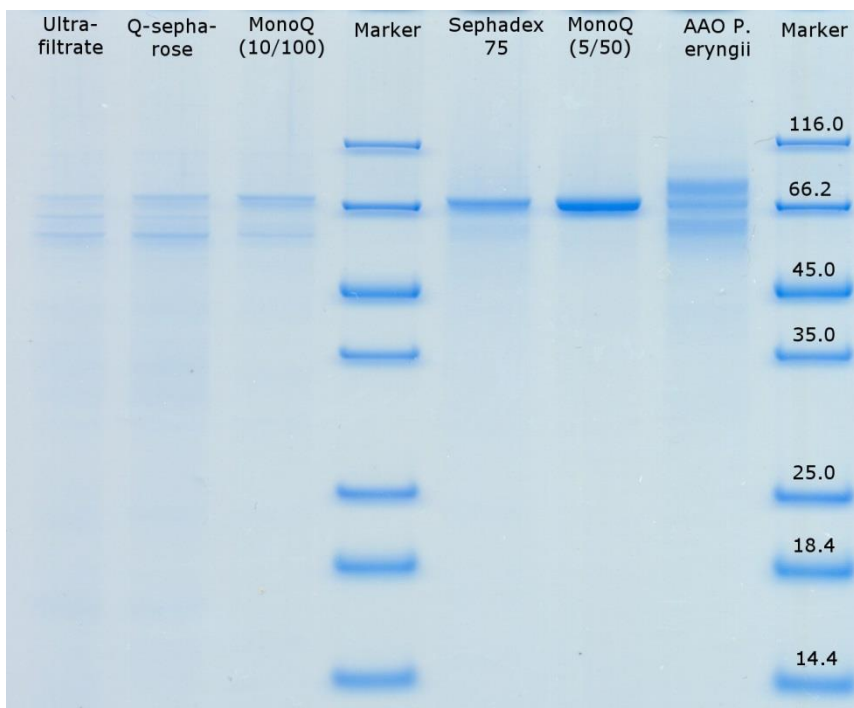


Fig. S7: SDS-PAGE of the different purification steps of AAO from *Pleurotus ostreatus* and purified AAO from *Pleurotus eryngii*; marker: Unstained Protein Molecular Weight Marker, Thermo Scientific; NuPAGE® Novex® Bis-Tris Mini-Gels 12%, Invitrogen; Conditions: 45 min, 200 V, 120 mA; staining with Novex® Colloidal Blue Stain Kit, Invitrogen

2.1 Analytical method

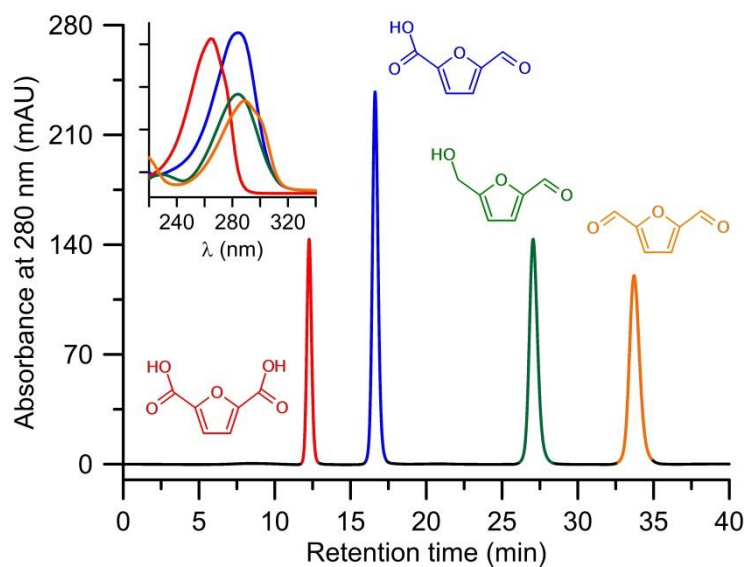


Fig. S 8: HPLC elution profile of a mixture containing HMF (green), DFF (orange), FFCA (blue) and FDCA (red); the inset displays the corresponding UV-spectra.

3.1 pH optimum of DFF oxidation

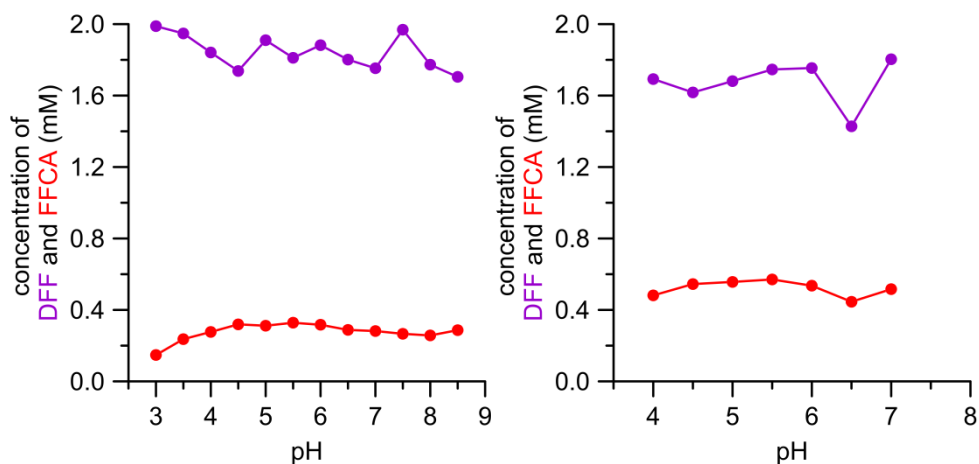


Fig. S9: pH dependencies of *PeryAAO* (A) and *PostAAO* (B) for DFF conversion. Violet curve – DFF concentration; red curve - FFCA concentration

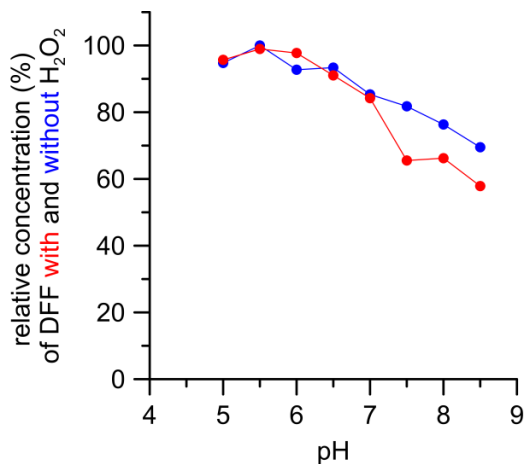


Fig. S10: pH dependency of DFF conversion catalyzed by GAO. Blue curve – relative concentration of DFF with H_2O_2 ; red curve – relative concentration of DFF without H_2O_2

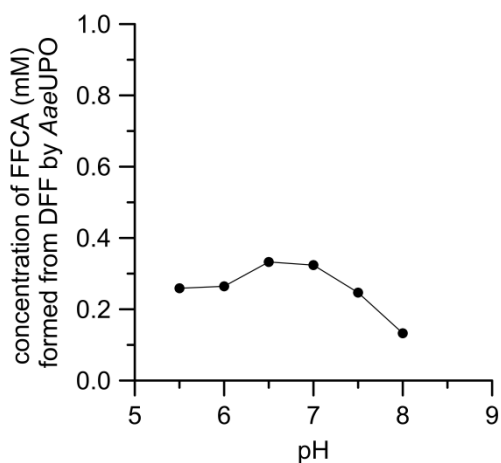


Fig. S11: pH dependent DFF oxidation catalyzed by *AaeUPO*. Black curve – DFF concentration

3.2 Calculation of apparent kinetic constants

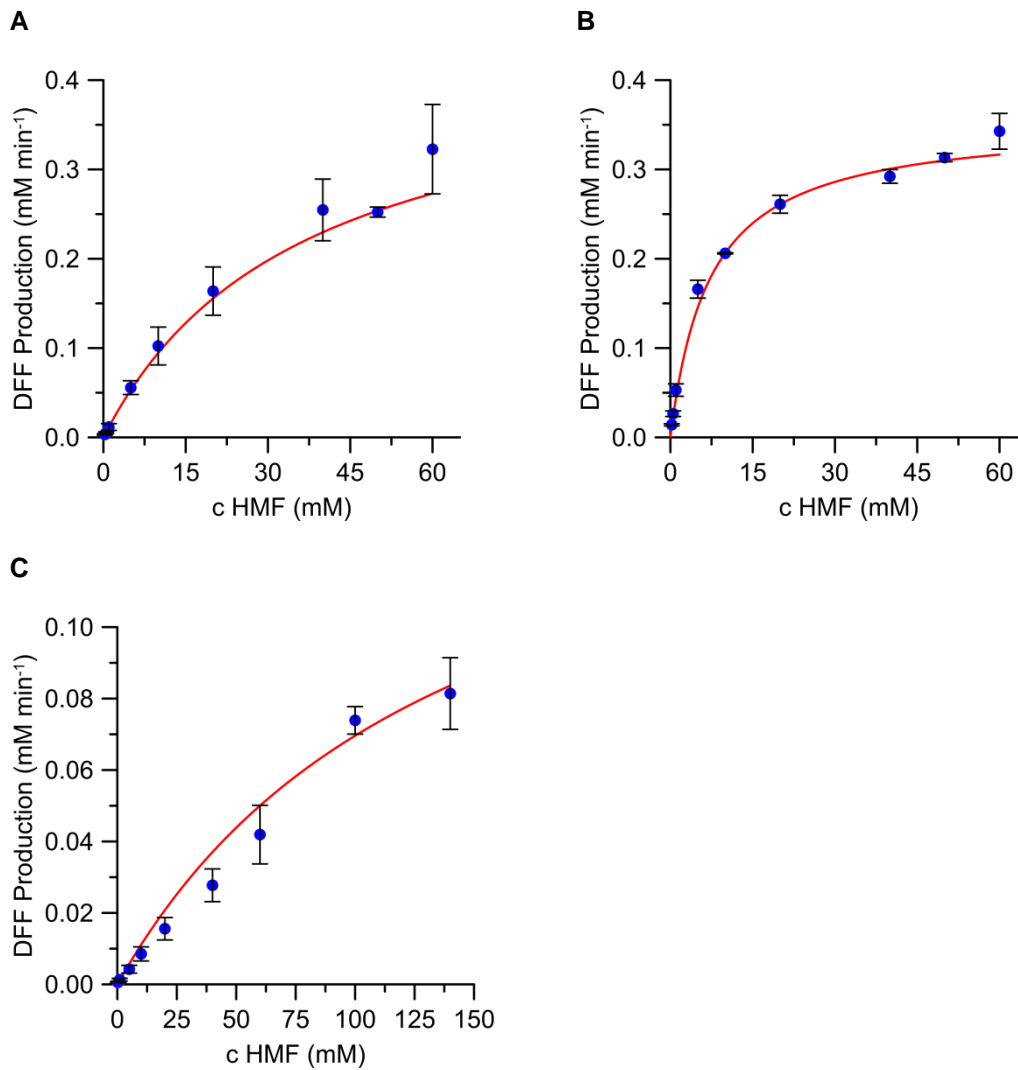


Fig. S12: Michaelis-Menten plots and their Lineweaver-Burk derivatives for the formation of DFF (from HMF) by *PeryAAO* (A), *PostAAO* (B) and *GAO* (C)

Setup:

pH: 2 mM HMF, 0.6 mg mL⁻¹ GAO, KP_i 30 mM, 1 μL NOVOZYMES Catalase (left), shaking for 2 h in 1.5-mL Eppendorf tubes

MM-Kin.: at pH 6.0, 4 μM GAO, stopped with Na azide (1 mM)

pH: 2 mM HMF, 60 μg mg mL AAO, KP_i 30 mM, 1 μL , shaking for 2 h in 1.5-mL Eppendorf-tubes

MM-Kin.: at pH 6.0, 2 μM AAO, stopped with Na azide (1 mM)

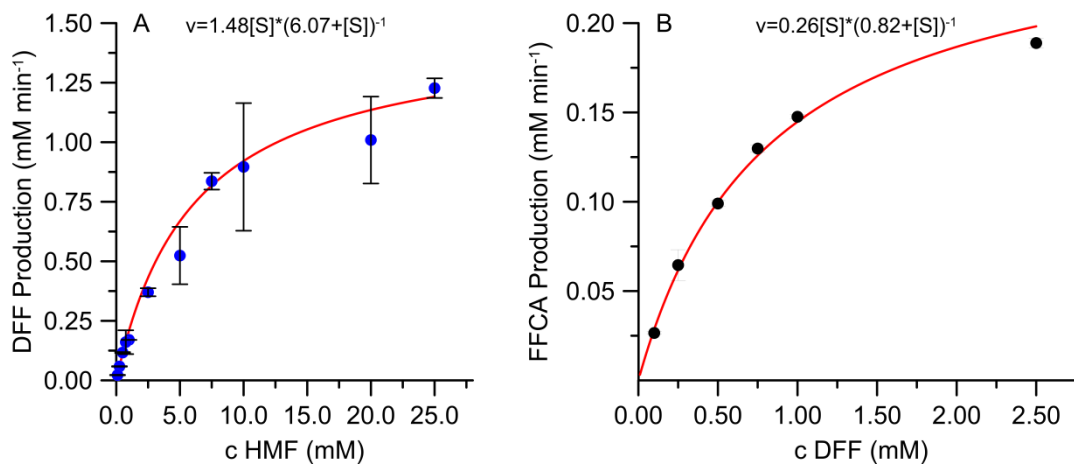


Fig. S13: Michaelis-Menten plots and their Lineweaver-Burk derivatives for the formation of DFF (A) and FFCA (B) by *AaeUPO*.

Setup MM-Kin.: at pH 6.0, 0.111 μ M *AaeUPO*, stopped with Na azide (1 mM)

3.3 AAO-dependent FFCA-oxidation with regard to varying H₂O₂ concentration

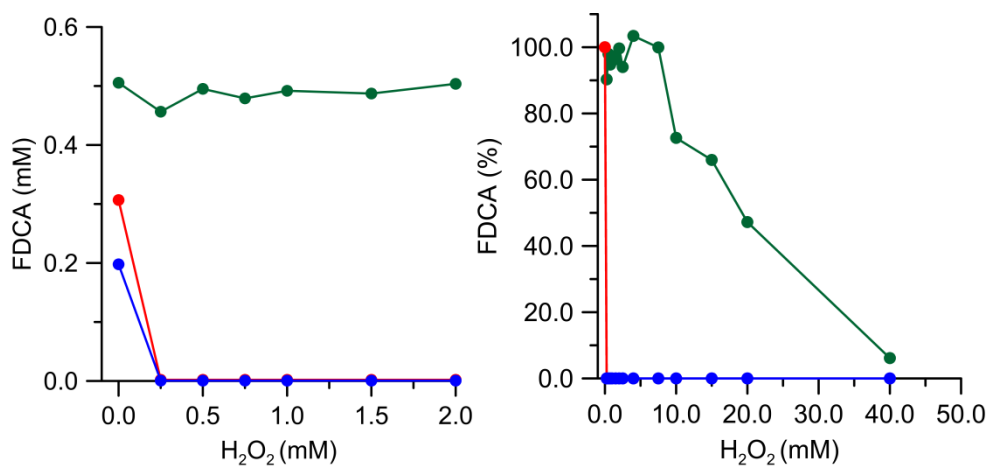


Fig. S14: FDCA formation catalyzed by *BaduAAO* (red), *PostAAO* (blue) and *PeryAAO* (green) with regard to different concentrations of H₂O₂ supplied (left) and relative FDCA production of *BaduAAO* (red), *PosAAO* (blue) and *PeryAAO* (green) (right).

Tab. S2: FDCA formation catalyzed by selected AAOs with regard to pH

	FDCA [mM]		
	pH 6	pH 7	pH 7.5
<i>PeryAAO</i>	0.008±0.00	1.706±0.21	0.903±0.09
<i>PostAAO</i>	0.004±0.00	0.012±0.00	0.004±0.00
<i>BaduAAO</i>	0.067±0.01	0.605±0.11	1.583±0.23